Human Embryonic and Induced Pluripotent Stem Cell–Derived Cardiomyocytes Exhibit Beat Rate Variability and Power-Law Behavior

Yael Mandel, MSc*; Amir Weissman, MD*; Revital Schick, BSc; Lili Barad, BSc; Atara Novak, MSc; Gideon Meiry, PhD; Stanislav Goldberg, BSc; Avraham Lorber, MD; Michael R. Rosen, MD; Joseph Itskovitz-Eldor, MD, PhD; Ofer Binah, PhD

Background—The sinoatrial node is the main impulse-generating tissue in the heart. Atrioventricular conduction block and arrhythmias caused by sinoatrial node dysfunction are clinically important and generally treated with electronic pacemakers. Although an excellent solution, electronic pacemakers incorporate limitations that have stimulated research on biological pacing. To assess the suitability of potential biological pacemakers, we tested the hypothesis that the spontaneous electric activity of human embryonic stem cell–derived cardiomyocytes (hESC-CMs) and induced pluripotent stem cell–derived cardiomyocytes (iPSC-CMs) exhibit beat rate variability and power-law behavior comparable to those of human sinoatrial node.

Methods and Results—We recorded extracellular electrograms from hESC-CMs and iPSC-CMs under stable conditions for up to 15 days. The beat rate time series of the spontaneous activity were examined in terms of their power spectral density and additional methods derived from nonlinear dynamics. The major findings were that the mean beat rate of hESC-CMs and iPSC-CMs was stable throughout the 15-day follow-up period and was similar in both cell types, that hESC-CMs and iPSC-CMs exhibited intrinsic beat rate variability and fractal behavior, and that isoproterenol increased and carbamylcholine decreased the beating rate in both hESC-CMs and iPSC-CMs.

Conclusions—This is the first study demonstrating that hESC-CMs and iPSC-CMs exhibit beat rate variability and power-law behavior as in humans, thus supporting the potential capability of these cell sources to serve as biological pacemakers. Our ability to generate sinoatrial-compatible spontaneous cardiomyocytes from the patient's own hair (via keratinocyte-derived iPSCs), thus eliminating the critical need for immunosuppression, renders these myocytes an attractive cell source as biological pacemakers. **(*Circulation*. 2012;125:883-893.)**

Key Words: heart rate ■ induced pluripotent stem cells ■ pacemaker, artificial ■ stem cells

Impulse initiation in the normal heart is the province of the sinoatrial node in which families of ionic currents and underlying clock mechanisms contribute to the pacemaker potential. In a variety of settings in which physiological pacing fails, therapy relies on electronic pacemakers. Although these are an excellent therapy, their inherent shortcomings such as inadequate autonomic control have stimulated the search for alternatives.[1–3] Biological pacemakers represent a promising prospect.

Editorial see p 856
Clinical Perspective on p 893

Three major approaches have been used to fabricate biological pacemakers.[1–4] In the first approach, viral vectors are used to deliver genes to regions of the heart. The result is a pacemaker potential leading to spontaneous impulse initiation in the region of gene administration. The second approach is the use of human embryonic stem cells (hESCs) or

Received May 24, 2011; accepted December 12, 2011.

From the Sohnis Family Stem Cells Center (Y.M., R.S., L.B., A.N., G.M., S.G., J.I.-E., O.B.), Rappaport Family Institute for Research in the Medical Science (Y.M., R.S., L.B., A.N., G.M., S.G., O.B.), and Ruth and Bruce Rappaport Faculty of Medicine (Y.M., A.W., R.S., L.B., A.N., G.M., S.G., A.L., J.I.-E., O.B.), Technion–Israel Institute of Technology, Haifa, Israel; Departments of Pediatric Cardiology (A.L.) and Obstetrics and Gynecology (A.W., J.I.-E.), Rambam Health Care Campus, Haifa, Israel; and Department of Pharmacology, College of Physicians and Surgeons of Columbia University, New York, NY (M.R.R.).

*Y. Mandel and Dr Weissman contributed equally to this article.

The online-only Data Supplement is available with this article at http://circ.ahajournals.org/lookup/suppl/doi:10.1161/CIRCULATIONAHA.111.045146/-/DC1.

Correspondence to Ofer Binah, PhD, Department of Physiology, Ruth and Bruce Rappaport Faculty of Medicine, PO Box 9649, Haifa, 31096 Israel. E-mail binah@tx.technion.ac.il

Circulation **is available at http://circ.ahajournals.org** **DOI: 10.1161/CIRCULATIONAHA.111.045146**

induced pluripotent stem cells (iPSC) grown along a cardiac lineage and manifesting electrophysiological properties similar to those of sinoatrial node cells. The third approach is to use combined gene/cell therapies incorporating adult human mesenchymal stem cells as a platform for generating spontaneous activity and/or expressing pacemaker currents, such as the funny current (I_f).

Initial proof of concept has given way to attempts to optimize biological pacemakers so that their function as generators of stable basal rates and of brisk autonomic responses is manifested over long intervals. Importantly, the functional features of the prototypical biological pacemaker, the sinoatrial node, are not limited to simple automaticity. Rather, the normal node has an organized rhythm that is stable over time and is integrated with host myocardium in such a way that it can impose a dominant rhythm on the atrial (and cardiac) substrate. Furthermore, it has autonomic responsiveness and shows specific responses to rate-modifying drugs (eg, I_f blockers). It is likely desirable that at least a subset of fabricated biological pacemaker would function much like the sinoatrial node. To achieve this, it would be useful to acquire additional understanding of the intrinsic firing patterns of cell types proposed for biological pacemakers with the sinoatrial node used as an operational standard.

Although previous studies have demonstrated that hESC-derived cardiomyocytes (hESC-CMs) and iPSC-derived cardiomyocytes (iPSC-CMs) fire spontaneously and respond to autonomic agonists and antagonists and to rate-modifying agents,[5–8] their dynamic firing pattern characteristics and their stability have not been reported. Indeed, only the beat rate variability (BRV) characteristics and stability of human mesenchymal stem cell–derived biological pacemakers loaded with the *HCN2* gene have been reported, and these studies have been performed only in the heart in situ.[9] Thus, the goal of this work is to determine the dynamic firing pattern properties, represented by BRV characteristics and fractal-like behavior, of hESC-CMs and iPSC-CMs and to compare them with pacemaker properties.

In designing the study, we considered the following: A key feature of the human sinoatrial node is that heart rate variability (HRV) exhibits self-similar fractal-like oscillations that contribute to its complexity.[10–12] In considering the fractal properties of stem cell–derived pacemakers in light of those of the sinoatrial node, we refer specifically to long-term oscillations in rhythmic variability that repeat on multiple time scales. To determine whether hESC-CMs and iPSC-CMs feature the intrinsic dynamic properties that may qualify them as candidates for biological pacemaker substitutes for sinoatrial node, we used nonlinear and dynamic analysis methods, which are used to analyze HRV.[10–12]

On the basis of the abovementioned considerations, we tested the hypothesis that the hESC-CMs and iPSC-CMs pacemaker cells exhibit BRV and power-law behavior similar to those of the denervated sinoatrial node. We compared the electrogram properties of hESC-CMs and iPSC-CMs, determined whether the BRV exhibits fractal behavior, estimated whether 1 of these 2 cell types is more similar than the other to sinoatrial node on the basis of beat rate characteristics, and established whether the age of the culture is a factor in the organization of the BRV characteristics.

Methods

Generation of hESC-CMs and iPSC-CMs

hESC-CMs were generated from clones H9.2 and iPSC-CMs from human hair–derived keratinocytes as previously described and as detailed in the online-only Data Supplement.[5,8,13,14] For iPSC generation, 30 000 keratinocytes prepared from 10 hairs were seeded on an inactivated 3T3 feeder layer supplemented with green medium on day 1.[13,14] On the next day, 293T cells were transfected with lentiviral plasmids to generate the lentiviral vector harboring the STEMCCA cassette. Importantly, we found that efficient excision of the lentiviral vector leaves the iPSCs free of transgene integration and enables enhanced cardiomyocyte contraction.[14] The contracting areas in the embryoid bodies were carefully dissected out by microscalpel and transferred to fibronectin (1:20)-coated microelectrode arrays (MEAs).

Data Recording and Processing

Extracellular electrograms were recorded from spontaneously contracting EBs with the MEA setup (Multi Channels Systems, Reutlingen, Germany) as previously described and detailed in the online-only Data Supplement.[15] The temperature of the MEA was kept at 37 ± 0.1°C by means of a temperature-maintaining system.[15] For the 8-hour recordings (long-term experiments), the MEAs were saturated with a gas mixture consisting of 5% CO_2 and 95% air.

Statistical Analysis

From each time point in which the electric activity was measured, we analyzed 10 consecutive electrogram complexes for activation spike amplitude, activation duration, activation-repolarization interval, and interbeat intervals (IBIs).[15] Activation times were acquired from extracellular action potentials by the derivative method (dV_e/dtmin), recording the time at which the derivative reached its maximal negative deflection.[15] In Figures 1, 2, and 5 through 7, the changes in a particular parameter versus time and the differences between the experimental groups were analyzed by fitting a linear mixed-effects regression model, taking into account the repeated-measures data structure.[16] The comparison of changes versus time between hESC-CMs and iPSC-CMs was performed by fitting a mixed-effects model with time, cell type, and their interaction as fixed effects. A value of $P<0.05$ was considered significant. In Figure 4, we performed 2-way ANOVA followed by the Holm-Sidak post hoc test. The comparisons were designed to answer 2 questions: Is there a significant difference between the 2 cell types (in all the treatments), and is there a significant difference between each treatment? All treatments were compared with each other in both cell types, and the *P* values refer to both cell types. All reported *P* values resulted from the Holm-Sidak test. This test is used for both pairwise comparisons and comparisons with a control group. It is more powerful than the Tukey and Bonferroni tests and consequently is able to detect differences that these other tests do not detect.

Power-Law Analyses

Beat rate fluctuations exhibit self-similar power-law correlations over a wide range of time scales from seconds to multiple hours.[17] The scaling exponents associated with these power-law correlations were reported to be altered during different physiological or pathological states, illness, and aging,[18–22] thus reflecting the global underlying mechanisms of cardiac regulation. Although the slope of the log power on log frequency regression line in healthy individuals has a β value (see below) of ≈ -1, certain disease states can cause significant alterations of this β value.[18–20] The recorded data were analyzed by computing the power spectrum of all IBIs. Next, a robust line-fitting algorithm of log power (power spectral density) versus log frequency (f) was applied, and the slope of this line, denoted β, was calculated. The short recordings permitted examination of the power spectrum over 2 decades (10^{-2} to 1 Hz) and the

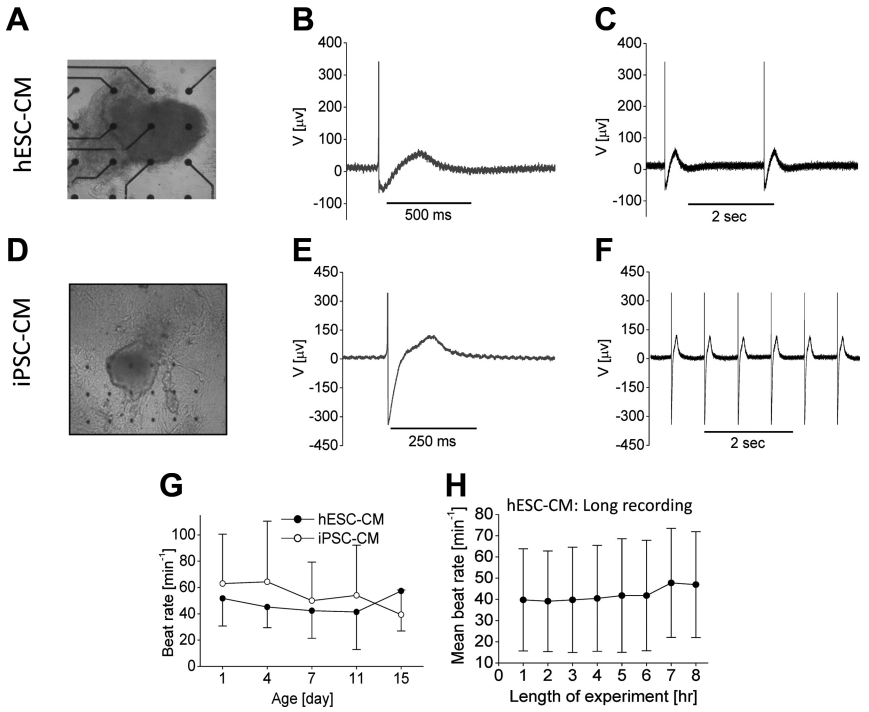

Figure 1. The spontaneous electric activity of human embryonic stem cell–derived cardiomyocytes (hESC-CMs) and induced pluripotent stem cell–derived cardiomyocytes (iPSC-CMs) cultures. **A** and **D**, hESC-CMs and iPSC-CMs clusters plated on top of the microelectrode array bath. Activation spikes and repolarization waves were recorded in hESC-CMs (**B** and **E**) and iPSC-CMs cultures. **B** and **E** show electrograms (from **C** and **F**) recorded on a faster time scale. **G** and **H**, The mean beat rate in the short- and long-term experiments, respectively. **G**, The mean beat rate was similar in hESC-CMs and iPSC-CMs and was steady over time in both groups: $P=0.52$, $P=0.64$, and $P=0.50$ for the interaction, time, and type analyses, respectively. Number of observations=5 to 6 on days 1 to 11 and 3 to 4 on day 15. Total observations=28 hESC-CMs and 25 iPSC-CMs. **H**, The mean beat was stable during the 8-hour recording session ($P=0.64$). n=4 embryoid bodies.

long recordings of 4 decades (10^{-4} to 1 Hz). A power law was assumed to be present if $r>0.85$.[23,24]

Detrended Fluctuation Analysis

Detrended fluctuation analysis (DFA) quantifies the intrinsic fractal-like correlation properties of dynamic systems with nonstationary signals.[25] The root mean square fluctuations of the integrated and detrended data time series were calculated in windows of different sizes and then plotted against the window size on a log-log scale. In the presence of scaling, the slope that relates log fluctuation to log window size is linear and describes the self-similarity and fractal-like correlation properties of the signal. As a result of the crossover phenomenon frequently observed in the regression line, α, it is customary to split the linear regression line into 2 distinct regions: $\alpha 1$ and $\alpha 2$ (or short term and long term, respectively).[26] Therefore, we calculated the short-term DFA $\alpha 1$ (4–16 beats) and the long-term DFA $\alpha 2$ (16–64 beats) scaling exponents. When $\alpha=0.5$, there is no correlation, and the signal consists of white noise; if $\alpha=1.5$, the signal is a random walk (brownian motion); if α is >0.5 and <1.5, there are positive correlations (Large IBIs are more likely to be followed by large intervals; small IBIs, by small intervals). A scaling exponent of ≈ 1 corresponds to 1/f (power-law) fluctuations.[11]

Poincaré Plot

The Poincaré plot is a chart in which each R-R interval is plotted against its predecessor and displays the correlation between consecutive intervals in a graphic manner. The quantitative analysis of the plot is achieved by fitting an ellipse to the plot with its center coinciding with the centroid of the ellipse (the point of the average R-R IBI) and adjusting 2 perpendicular lines traversing through the centroid. The longitudinal line, which is designated SD2, represents the long-term variability of the data (reflecting the SD of the IBIs), whereas the perpendicular line, designated SD1, represents the short-term beat-to-beat variability of the data[27] (analogous to the SD of successive differences of IBI or its root mean square). Poincaré plot analysis, which has been used in several clinical situations such as sinus node dysfunction,[28,29] enables us to visually identify the dynamic state of the system.

Phase-Space Reconstruction

The term phase space refers to an n-dimensional space defined by n parameters that identifies the state of the system at a given time. According to the Takens theorem,[30] it is possible to construct a phase-space trajectory of a system from a single scalar time series by composing its vectors with the method of time-delay coordinates. Analysis of time series by phase space can be used to identify hidden dynamic information embedded in the time series that may help us understand physiological or pathological mechanisms (eg, ischemic heart changes and other cardiac pathologies).[28,29,31] A 2-dimensional phase portrait of the IBIs was constructed from the original time series plotted against itself with a small time delay (τ).

Results

Experimental Model and Protocols

The electric activity of hESC-CMs and iPSC-CMs plated on MEAs was monitored for 15 days. To this end, MEAs were removed from the incubator on days 1, 4, 7, 11, and 15, and 10-minute recording sessions at 37°C were performed. After the recording, MEAs were returned to the incubator. Because of the small size of the contracting EBs, electrograms were usually recorded from <10 electrodes (Figure 1A and 1D). As shown in Figure 1, electrograms demonstrating robust activation spikes and repolarization waves were recorded from hESC-CMs and iPSC-CMs.

Spontaneous Beat Rate and the Electrogram Properties of hESC-CMs and iPSC-CMs

Using a dedicated MATLAB software package specifically constructed according to our needs, we generated the IBI time series for each of the 10-minute recordings, from which we calculated the mean IBI and mean beat rate. This analysis showed (Figure 1G) that the mean beat rate was similar in hESC-CMs and iPSC-CMs and was steady in both groups throughout the 15-day follow-up period. Because monitoring the same cultures for 15 days dictated that MEAs be removed from the incubator for $\approx$10 minutes, it was important to confirm that the number of recorded beats was sufficient for a reliable BRV analysis.[23,24] To validate the reliability of

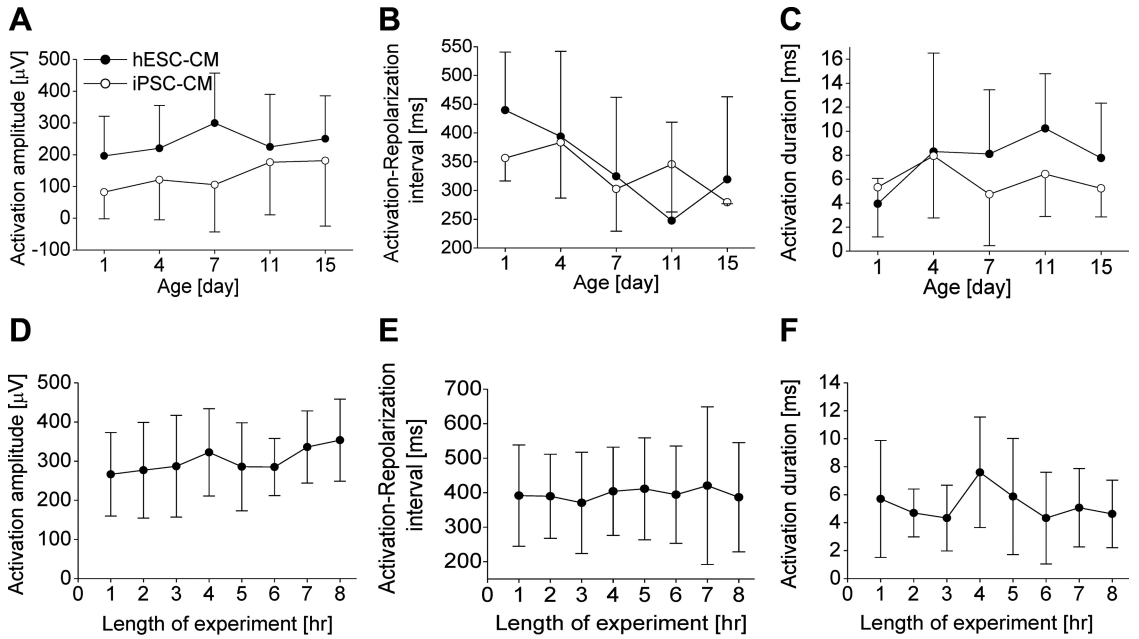

Figure 2. Electrogram properties in the short-term (human embryonic stem cell–derived cardiomyocytes [hESC-CMs] and induced pluripotent stem cell–derived cardiomyocytes [iPSC-CMs]) and long-term (hESC-CMs) experiments. Activation amplitude (**A**) and activation duration (**C**) were similar in both groups and stable during the recording session: $P=0.49$ and $P=0.43$ (for **A** and **C**, respectively), $P=0.31$ and $P=0.45$, and $P=0.09$ and $P=0.88$ for the analyses of interaction, time, and type, respectively. **B**, Activation-repolarization interval (ARI) was longer in hESC-CMs than in iPSC-CMs and stable during the recording session: $P=0.93$, $P=0.57$, and $P=0.025$ for the interaction, time, and type analyses, respectively. In the 8-hour experiments (n=3–4 embryoid bodies), the activation amplitude (**D**), ARI (**E**), and activation duration (**F**) were stable over time: $P=0.32$, $P=0.22$, and $P=0.56$, respectively.

10-minute recordings for the analyses, we compared the electrogram properties and BRV characteristics of the 10-minute recordings with those of 8-hour recordings performed in 4 hESC-CMs cultures. In these experiments, spontaneous activity was recorded during 8 hours in MEAs maintained (outside the incubator) at 37°C and equilibrated with a gas mixture of 5% O_2 and 95% air. As shown in Figure 1H, the mean beat rate, which was stable ($P=0.64$) during the 8-hour recording session, was compatible with the mean beat rates of short-term recordings, thus validating the reliability of the 10-minute recording. Next, we compared the electrogram properties of the 2 cell types. Activation amplitude (Figure 2A) and activation duration (Figure 2C) were similar in both groups and stable during the recording session. In contrast, the activation-repolarization interval (Figure 2B) was longer in hESC-CMs than in iPSC-CMs and stable during the recording session. To further validate the short-term recordings, the electrogram properties were analyzed in the 8-hour experiments. As shown in Figure 2D through 2F, all the parameters were stable in the course of the experiment and similar to those of the 10-minute experiments, further supporting the reliability of the short-term recordings.

The Chronotropic Response of hESC-CMs and iPSC-CMs to Autonomic Neurotransmitters

To test whether hESC-CMs and iPSC-CMs pacemaker properties are compatible with the sinoatrial node, we determined the chronotropic responsiveness to isoproterenol and carbamylcholine (see details in the online-only Data Supplement). As illustrated by the representative recordings (Figure 3) and the summary of these experiments (Figure 4A), isoproterenol increased the beat rate and metoprolol blocked this stimulatory effect in both cell types. Furthermore, in both cell types, the beat rate was decreased similarly by carbamylcholine, an expected inhibitory effect blocked by the presence of atropine (Figure 4B).

The Fractal Self-Similarity of the BRV

A time series can be considered self-similar or fractal if comparable fluctuations over multiple time scales can be identified. Our hypothesis was that if hESC-CMs and iPSC-CMs have fractal properties and obey the same physical rules as pacemaker cells in the sinoatrial node, then they may provide an adequate substitute for abnormally functioning sinoatrial pacemakers. To determine the presence of self-similarity in the IBI time series, we used DFA. Figure 5A and 5D depict examples calculating $\alpha 1$ and $\alpha 2$ in 4-day-old hESC-CMs and in 18-day-old iPSC-CMs, respectively. The linear relation between F(n) and n on a double-logarithmic scale indicates the presence of self-similarity. The $\alpha 1$ values (Figure 5B) were similar in both groups and stable during the follow-up period. As for $\alpha 2$ (Figure 5E), although no difference was found between the groups, $\alpha 2$ increased with time in both cell types. In agreement with previous results, the self-similarity of the 8-hour-recording DFA scaling exponents (Figure 5C and 5F) was similar to that of the short recordings, further validating the time-series analysis of the short recording protocol. Specifically, both $\alpha 1$ and $\alpha 2$ were stable during the 8-hour recording. These results corroborate the fractal nature of hESC-CMs and iPSC-CMs, which appears to be an inherent feature of these cells.

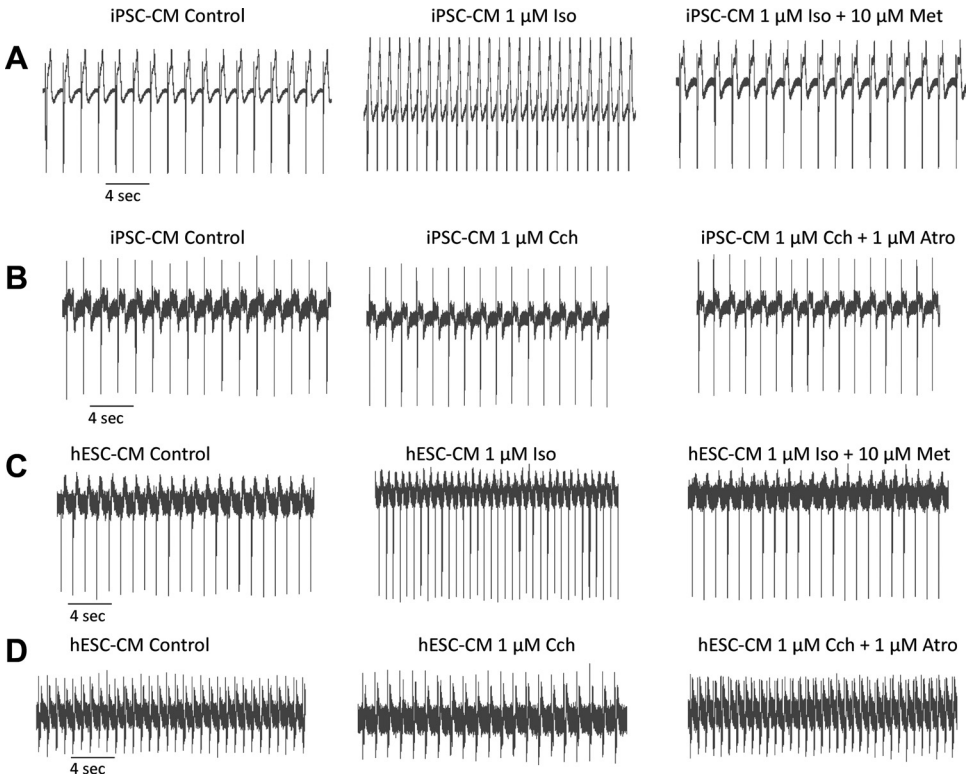

Figure 3. The chronotropic response of human embryonic stem cell–derived cardiomyocytes (hESC-CMs) and induced pluripotent stem cell–derived cardiomyocytes (iPSC-CMs) to autonomic neurotransmitters. Representative electrograms recorded from iPSC-CMs (**A** and **B**) and hESC-CMs (**C** and **D**) in the absence or presence of the β-adrenergic agonist isoproterenol (Iso; followed by isoproterenol plus metoprolol [Met]) or the muscarinic agonist carbamylcholine (Cch; followed by carbamylcholine plus atropine [Atro]).

Spectral Analysis and Power-Law Behavior

To determine the spectral content of the IBI time series, fast Fourier transform analysis was performed. For each of the 10-minute recordings, the total power of IBI variability corresponds to the sum of the power spectral density in the following spectral bands: ultralow frequency, <0.003 Hz; very low frequency, 0.003 to 0.04 Hz; low frequency, 0.04 to 0.15 Hz; and high frequency, 0.15 to 0.4 Hz.[31] For each recording, the total power in each spectral band was calculated. Subsequently, the relative power of the spectrum in each band was derived as the ratio between the individual band and the total power (100%). In 50 of the 62 short

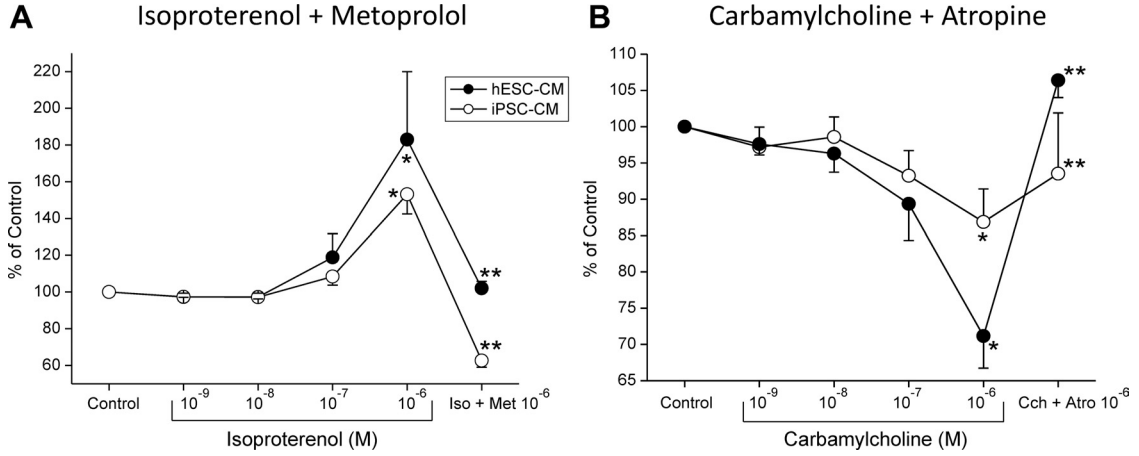

Figure 4. The chronotropic response of human embryonic stem cell–derived cardiomyocytes (hESC-CMs) and induced pluripotent stem cell–derived cardiomyocytes (iPSC-CMs) to autonomic neurotransmitters. **A**, The effect of isoproterenol on the beat rate of iPSC-CMs and hESC-CMs and the blocking effect of the β-blocker metoprolol. The effect of isoproterenol was statistically significant (*$P<0.001$) and similar in both cell types ($P=0.277$). Metoprolol significantly (**$P=0.009$) decreased the effect of 10^{-6} mol/L isoproterenol and was similarly effective in both cell types ($P=0.386$). **B**, The effect of carbamylcholine on the beat rate of iPSC-CMs and hESC-CMs and the inhibitory effect of the cholinergic blocker atropine. The effect of carbamylcholine was statistically significant (*$P<0.001$) and similar in both cell types ($P=0.076$). Atropine significantly (**$P=0.009$) decreased the effect of 10^{-6} mol/L carbamylcholine and was similarly effective in both cell types ($P=0.117$). Results (mean±SEM) are expressed as percent change from control beat rate. n=3 embryoid bodies in each cell type. For details, see the online-only Data Supplement.

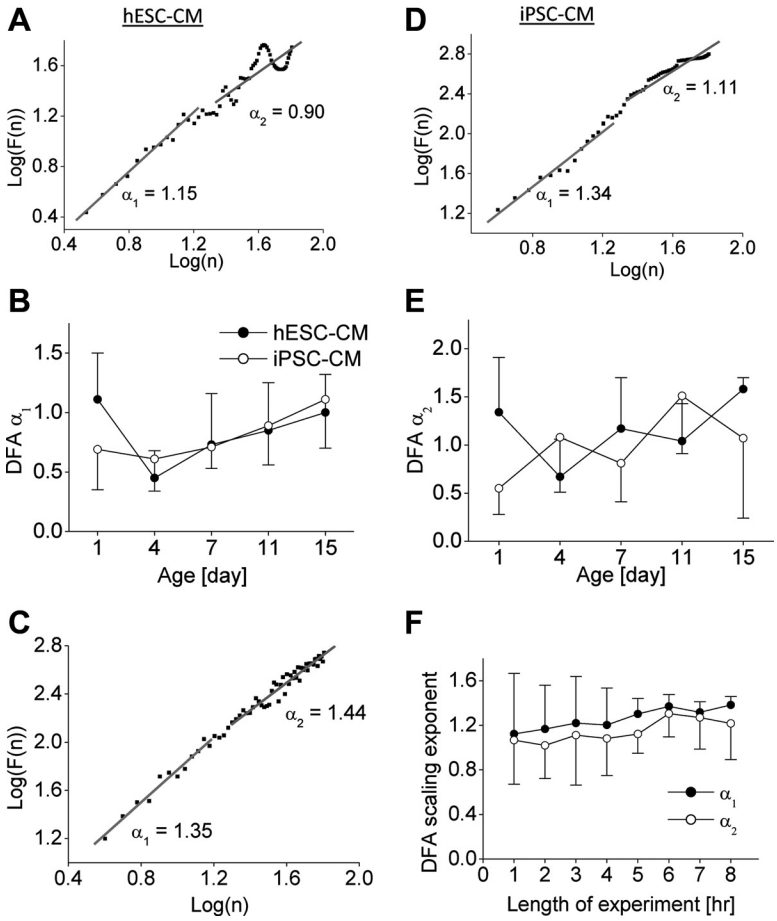

Figure 5. Analysis of self-similarity of the beat rate time series with detrended fluctuation analysis (DFA) in short- and long-term experiments. **A** and **D**, DFA calculations for a representative short-term human embryonic stem cell–derived cardiomyocytes (hESC-CMs) culture (day 4) and a representative induced pluripotent stem cell–derived cardiomyocytes (iPSC-CMs) culture (day 18), respectively. The plot of F(n) over n on a double-logarithmic plot shows a linear relation from which the short-term scaling exponent (α1) and the long-term scaling exponent (α2) were calculated. **B**, Values of α1 were similar in both groups and stable during the experiments: P=0.20, P=0.45, and P=0.88 for the interaction, time, and type analyses, respectively. **E,** Values of α2 were similar in both groups (P=0.20 and P=0.188 for the interaction and type analyses, respectively) and increased with time in both groups (P=0.05). **C**, DFA calculations for a representative long-term hESC-CMs culture. **F**, Values of α1 and α2 in the 8-hour experiments (n=4 embryoid bodies) were stable during the 8-hour recording (P=0.25 and P=0.55, respectively).

recordings, >90% of the spectral power was concentrated in the ultralow-frequency and very-low-frequency bands. Because several previous studies[22,23] reported that most of the spectral power in cultured neonatal rat ventricular myocytes is concentrated in the ultralow-frequency and very-low-frequency bands, we focused the additional analyses on these bands.

Power-Law Analyses

A common means for quantifying self-similar fractal behavior is by calculating the scaling relationship of the measured parameter during multiple time scales, which yields power-law relationships.[23,24,32,33] Figure 6 depicts the procedure for calculating the power-law exponent, β. In these representative examples (Figure 6A and 6B), the β values for hESC-CMs and iPSC-CMs were −1.9 and −2.1, respectively. A summary of this analysis (Figure 6C) shows that the β values were similar in both culture types and constant throughout the follow-up period. To address whether the spectral analysis of the 10-minute short recordings yielded accurate β values, we analyzed the 8-hour experiments, which yielded 4 decades of frequencies (Figure 6D). Hence, for the frequencies of interest in clinical studies (10^{-2}–10^{-4} Hz), an 8-hour period is more than adequate. As shown in Figure 6C and 6E, we found that the β values were similar in the 10-minute and 8-hour recordings and stable during both the short-term and long-term experiments. With regard to the relevance of these findings to the sinoatrial node, a healthy subject has a power-law slope of ≈−1, whereas subjects with disease have steeper slopes.[18,19,33] For example, the denervated heart (eg, after heart transplantation) can reach slopes of ≈−2.[19]

Assessing Beat Rate Dynamics With a Poincaré Plot

To obtain an additional quantitative measure of the temporal evolution of the BRV, we generated Poincaré plots for the 10-minute recordings, which enabled us to visualize the short- and long-term variability of the IBI. In the Poincaré plot, IBI_{n+1} is plotted against IBI_n, thus creating a scattered mass of points in a 2-dimensional array. This group of points is then fitted with an ellipse providing 2 quantitative indexes; the SD of the short-axis (SD1) and long-axis (SD2) IBI variability of the cloud. As depicted in Figure 7A and 7B, in the Poincaré plots of 2 representative experiments, the SD1 and SD2 in hESC-CMs were 22.1 and 53.6, respectively, and in iPSC-CMs were 55.2 and 204.5, respectively; the shapes of these plots resemble those of human subjects showing the typical dispersion. In summary, as shown in Figure 7C and 7D, SD1 and SD2 were similar in hESC-CMs and iPSC-CMs and remained unchanged throughout the experiment.

Phase-Space Analysis

In the phase-space plot, the electrogram voltage at time n+1 is plotted against the preceding value at time n, thus providing an interpretation of the dynamic properties of the system. Figure 8 depicts the evolution of the phase-portrait pattern in

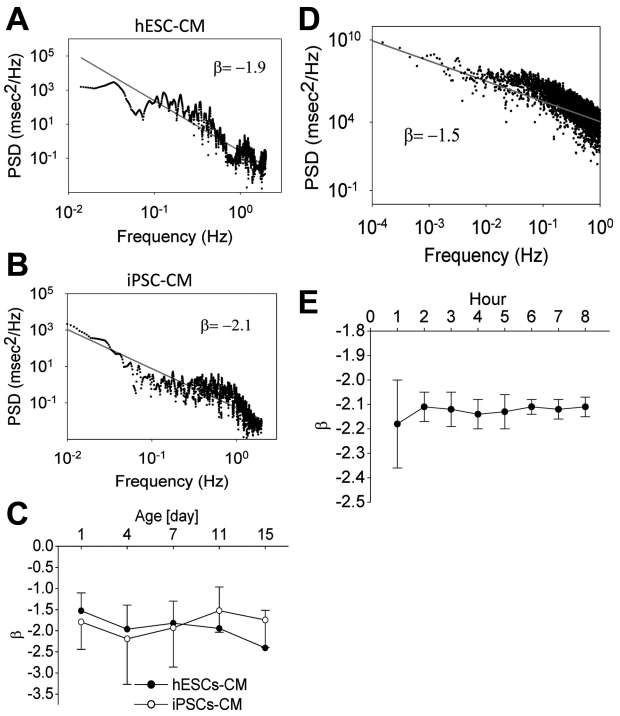

Figure 6. Power-law behavior of beat rate variability in short- and long-term recordings. Power spectral analysis performed with fast Fourier transform reveals a linear relationship between power spectral density and frequency on a double-logarithmic scale in representative human embryonic stem cell–derived cardiomyocytes (hESC-CMs; **A**) and induced pluripotent stem cell–derived cardiomyocytes (iPSC-CMs; **B**) cultures, both from day 15. The slope of the fitted regression line corresponds to the power-law exponent β. **C**, The same procedure was repeated for each of the short-term recordings, and β was averaged separately according to culture type. Values of β were similar in both groups and stable over time: $P=0.10$, $P=0.10$, and $P=0.88$ for the interaction, time and type analyses, respectively. **D**, An example of calculating β in the long-term experiment. **E**, A summary of the β values during the long-term experiment. Values of β were stable over time: $P=0.22$.

one hESC-CMs culture during the 15-day follow-up period. In this culture, on day 1 (on which contractile activity was first detected), the plot shows a disorganized electric pattern filling a certain space. As of day 4, a QRS-like electric activity forms, further developing with time into an organized pattern similar to those generated by human ECGs.[34] In some cultures, the evolution of the dynamic electric activity proceeded from an organized to a disorganized pattern, whereas in others, the pattern (either organized or disorganized) remained unchanged throughout the follow-up period.

Discussion

In this study, we tested the hypothesis that the spontaneous electric activity of hESC-CMs and iPSC-CMs exhibits BRV behavior comparable to that of human HRV, rendering these cells potential sinoatrial node substitutes in specific clinical settings. This hypothesis was based on the premise that a biological pacemaker proposed as a sinoatrial node replacement not only should fire spontaneously but also should resemble the sinoatrial node in its BRV and fractal behavior, enabling an adaptable response to changing conditions. Our major findings were the following. First, the mean beat rate of hESC-CMs and iPSC-CMs was stable throughout the 15-day follow-up period and similar in both cell types. Second, hESC-CMs and iPSC-CMs exhibited intrinsic BRV and fractal behavior. Third, in both hESC-CMs and iPSC-CMs, isoproterenol increased and carbamylcholine decreased the beating rate. Metoprolol and atropine blocked the chronotropic effects of isoproterenol and carbamylcholine, respectively. These findings (discussed below in detail) suggest that (1) hESC-CMs and iPSC-CMs resemble pacemaker cells; (2) although both cell types go through a process of "maturation" or "organization," it relates only to their dynamic-fractal aspect (ie, they beat spontaneously from day 1 but somehow become organized (not all cultures) from a dynamic point of view and acquire their fractal nature only later on); and (3) the "trigger" is unique in its capability to spontaneously beat and adapt to changing conditions. This is in contrast to adult ventricular cells that lack such a capacity. This is the first study showing that hESC-CMs and iPSC-CMs exhibit BRV and fractal behavior as in humans, thus supporting the capability of these cell sources to serve as biological pacemakers.

The Electric Properties of hESC-CMs and iPSC-CMs and Chronotropic Autonomic Responsiveness

A plausible criterion for deciding if one cell type is superior to the other as a potential source for a biological pacemaker is the stability of the electrogram properties and beat rate over time in growing cultures. A comparison between hESC-CMs and iPSC-CMs showed that both cell types were electrically stable during the 15-day follow-up period and, importantly, that their beat rates (39–70 bpm) were within the (lower) range of the human heart rates. The beat rates measured in this study are similar to spontaneous rates reported for hESC-CMs by Kehat et al[35] (94±33 bpm; n=8) and Mummery et al[36] (35–90 bpm). Because the cultures were removed from the incubator every few days for a 10-minute recording session, it was important to show that the electrogram properties resemble those of cultures that were under steady-state conditions. That this is the case is indicated by the similarity of electrogram properties of the short-term and long-term experiments. Collectively, these experiments demonstrate that the cultures were electrically stable during the follow-up period and that one cell type is not advantageous over the other. The basis for the longer activation-repolarization interval in hESC-CMs was not accounted for in the present work and could result from several possibilities such as different proportions of cardiomyocytes composing the EBs. The compatibility of hESC-CMs and iPSC-CMs with sinoatrial node function is supported by the finding that the beat rate was increased by isoproterenol (the effect blocked by metoprolol) and decreased by carbamylcholine (the effect blocked by atropine). These key features, combined with the BRV, self-similarity, and power-law behavior (see below), demonstrate that both pacemaker sources are potential candidates for biological pacemakers.

BRV, Self-Similarity, and Power-Law Behavior

Self-Similarity and Fractality

A key feature of the human sinoatrial node is that HRV exhibits self-similar fractal-like oscillations.[10–12] This is de-

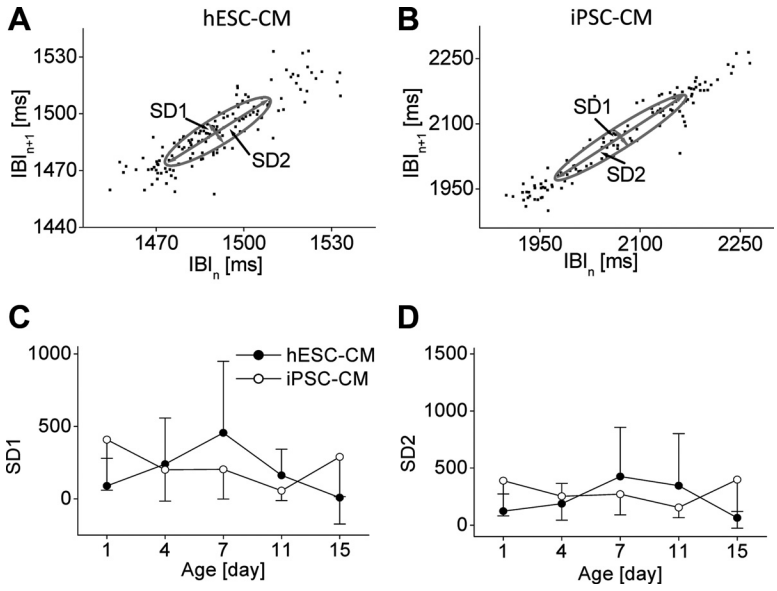

Figure 7. Poincaré plots of the beat rate variability in short-term recordings. Poincaré plots in representative human embryonic stem cell–derived cardiomyocytes (hESC-CMs; **A**) and induced pluripotent stem cell–derived cardiomyocytes (iPSC-CMs; **B**) cultures. See Methods for details. The minor axis (SD1) of the ellipse represents the SD of the short-term interbeat interval (IBI) variability, and the major axis (SD2) represents the SD of the long-term IBI variability. **C** and **D**, A summary of SD1 and SD2 values for both culture types. SD1 and SD2 did not differ between hESC-CMs and iPSC-CMs and remained stable during the 15-day follow-up period. For SD1, $P=0.42$, $P=0.44$, and $P=0.36$; for SD2, $P=0.39$, $P=0.81$, and $P=0.31$ for the interaction, time, and type analyses, respectively.

picted by the fractal-like feature of the beat rate time series and by the short-term and long-term DFA scaling exponents $\alpha 1$ and $\alpha 2$, which provide a quantitative measure of self-similarity. In agreement with the abovementioned electric properties, both hESC-CMs and iPSC-CMs exhibited similar scaling exponents, which were stable throughout the follow-up period (Figure 5). It is noteworthy that although hESC-CMs and iPSC-CMs grow in culture devoid of extra-

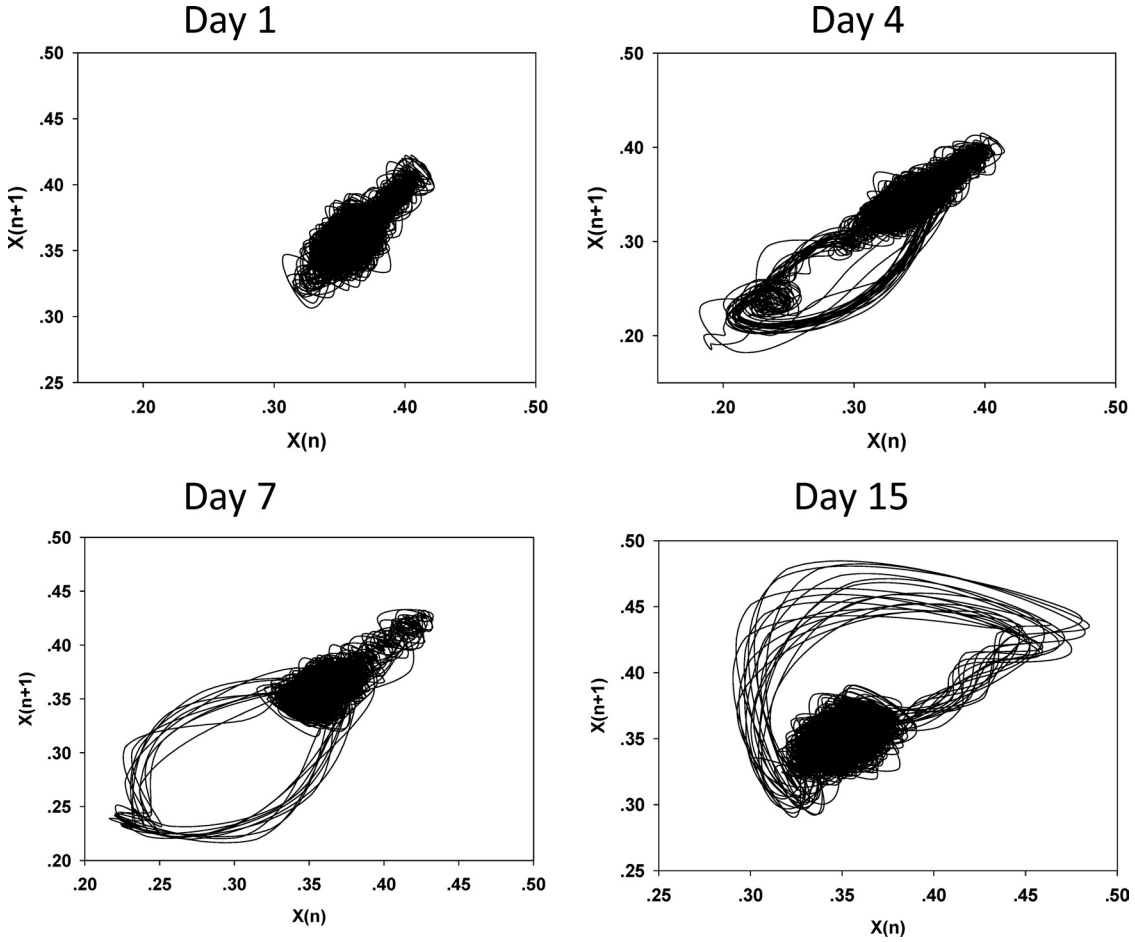

Figure 8. Phase-portrait display of the electrogram signal. Two-dimensional phase-space figure of a representative human embryonic stem cell–derived cardiomyocytes (hESC-CMs) culture during a 15-day follow-up. Day 1: a compact, dense, disorganized pattern. Day 4: the beginning of an organized QRS-like pattern formation. Day 7: the QRS pattern becomes more accentuated. Day 15: a fully organized (human-like) pattern.

cardiac influences, both share the feature of fractal behavior with the in situ sinoatrial node. This may be due to the intrinsic fractal properties of pacemaker cells, as was also hypothesized by others.[23,24]

Power-Law Behavior

In agreement with the self-similarity behavior of the BRV, we found that the IBI spectrum of both hESC-CMs and iPSC-CMs followed power-law relations, supporting the notion of intrinsic self-similarity properties of both cell types. The β values we found in the region of the very low and ultralow frequencies are similar to those reported in humans after heart transplantation[19] and confirm the fractal nature of these lines of contracting cells that follow the power-law rule. This also implies that this power-law behavior is an intrinsic feature of pacemaker cells, being devoid of extrinsic influences, and not necessarily a result of extracardiac factors such as the autonomic nervous system.

Poincaré Plot

The Poincaré plot displays the IBI versus the preceding interval, and the shape of this plot can be classified into several categories that can visually differentiate between healthy individuals and those with heart failure or arrhythmias and provide insights into the behavior of the automatic rhythm.[27,28] Because it was reported that the Poincaré plot shape and indexes are affected by the autonomic nervous system,[27] it was important to investigate the beat rate dynamics of cardiomyocytes isolated from external stimuli. The Poincaré plot analysis of IBIs of hESC-CMs and iPSC-CMs exhibited the typical cigar-shaped scatter of points, resembling a "human-like" dispersion of the IBIs. When considering these cells as candidates for biological pacemaker, this dynamic behavior of their activity is encouraging. Long-term recordings showed Poincaré plot indexes similar to those in short-term recordings, suggesting that the findings above also are valid for long-term continuous periods. Hence, the findings in neonatal rat ventricular myocytes[23,24] also support the notion that fractal-like behavior of the BRV originates from the inherent intrinsic properties of the pacemaker cells and does not require extracardiac factors such as the autonomic nervous system, which nonetheless would serve as modifiers.

Phase-Portrait Analysis

In the study of the dynamics of a system, it is possible to construct its state space from a single scalar measurement by applying the time-delay technique, thus achieving the topological equivalent of the original state space of the system.[30,31] This method is accomplished by plotting a single measurement, x(t), versus the following measurement with a small time delay, $x(t+\tau)$. This analysis was used to identify "hidden" information embedded in the fluctuations of the time series and to gain insights into the dynamics of the system that cannot be otherwise detected. Figure 8 depicts a 2-dimensional phase-space portrait of the electric signal time-series data from a hESC-CMs culture during the 15-day follow-up period. The dense, packed, complex pattern of trajectories that fill the space in a random manner on day 1 begins to form nested loops that resemble a "QRS-like" activity on day 4, and these loops with irregular transitions between them become more orderly as time advances. On day 15, an organized pattern is formed with loops that are limited to a well-defined space and with trajectories that are close to each other. Other cultures showed an inverse transition from an organized pattern to a disorganized pattern and eventually stopped beating. The importance of this dynamic representation of the signal is that it permitted the differentiation between mature organized cultures that resemble a human-like pattern of activity and cultures with an immature or disorganized activity pattern. It is noteworthy that by no other means was it possible to differentiate between these 2 types of activities because their morphology and time- and frequency-domain characteristics were similar. Hence, only by using nonlinear analysis methods could we differentiate and classify the dynamic behavior of the cardiomyocytes BRV into disorganized and organized classes. Therefore, this analytic tool can be added to the more common criteria for selecting the appropriate biological pacemaker.

HRV and Fractal Behavior of hESC-CMs and hESC-CMs Versus the Sinoatrial Node

Our findings that cardiomyocytes clusters devoid of extrinsic influence exhibit BRV and fractal behavior resembling those of the sinoatrial node create a level of complexity calling for further investigation. In the normal heart, HRV is thought to reflect dynamic coupling between the autonomic nervous system as a modulator and sinoatrial node pacemaker activity. In the denervated heart, on the other hand, where interplay of the autonomic system is abolished, the responses of heart rhythm dynamics suggest the presence of intrinsic cardiac regulatory mechanisms.[19] Similar dynamics has been also reported in spontaneously beating cardiomyocytes.[23,24] Although the power spectrum of the BRV was decreased at all frequencies (as reflected by the steep slope of the power-law regression line, ≈ -2), probably indicating the lack of autonomic inputs,[18] it still maintained its fractal, scale-invariant behavior. Although the nature of this phenomenon is unclear, it may be postulated that the momentary BRV of the cell clusters results from the summated interactions among different oscillators constituting the cell mass. This may explain why the beat rate is not constant and metronome-like but changes with each beat. Furthermore, it is assumed that in the embryonic cell mass, every cell is an independent dynamic oscillator in which a variety of simultaneous regulatory processes take place. These dynamic changes (eg, biochemical, structural) generate continuous variations in the electric properties of each single contracting cell, thus generating BRV. In this complex network of oscillators, electric variations take place constantly, and dominance of the pacemaker is shifted across these multiple cells, forming the network. This concept has been reported elegantly in cultures of neonatal rat cardiomyocytes by Ponard et al.[24] That study showed how stochastic or deterministic intracellular processes (enzymatic, metabolic, ion-channel turnover, etc) can be the origin of power-law behavior of beat rate. It was therefore concluded that these intrinsic properties of cardiac tissue are responsible for BRV in these cultures,

findings that were also confirmed in our cultures of human origin.

Conclusions

We have shown for the first time that human stem cell–derived cardiomyocytes from 2 different sources (hESC-CMs and iPSC-CMs) present BRV properties and power-law behavior similar to those observed in humans. These novel findings suggest that potential sources for biological pacemakers should be screened on the basis of not only their mere ability to fire spontaneously but also their inherent dynamic pacemaker properties. Our ability to generate sinoatrial-compatible spontaneous cardiomyocytes from the patient's own hair (via keratinocyte-derived iPSC),[14] thus eliminating the critical need for immunosuppression, renders these myocytes an attractive cell source as biological pacemakers.

Sources of Funding

This work was supported by the Israel Science Foundation, Ministry of Health–Chief Scientist, the United States-Israel Binational Science Foundation, the Rappaport Family Institute for Research in the Medical Sciences, and the Sohnis and Forman Families Stem Cells Center.

Disclosures

None.

References

1. Rosemblit N, Moschella MC, Ondriasa E, Gutstein DE, Ondrias K, Marks AR. Intracellular calcium release channel expression during embryogenesis. *Dev Biol*. 1999;206:163–177.
2. Rosen MR. Conference report: building a biologic pacemaker. *J Electrocardiol*. 2007;40(suppl):S197–S198.
3. Robinson RB, Brink PR, Cohen IS, Rosen MR. I(f) and the biological pacemaker. *Pharmacol Res*. 2006;53:407–415.
4. Rosen MR, Brink PR, Cohen IS, Robinson RB. Biological pacemakers based on I(f). *Med Biol Eng Comput*. 2007;45:157–166.
5. Dolnikov K, Shilkrut M, Gerecht-Nir S, Zeevi-Levin N, Ohayon D, Danon A, Itskovitz-Eldor, Binah O. Functional properties of human embryonic stem cell-derived cardiomyocytes: intracellular Ca^{2+} handling and the role of sarcoplasmic reticulum in the contraction. *Stem Cells*. 2006;24:236–245.
6. Caspi O, Itzhaki I, Kehat I, Gepstein A, Arbel G, Huber I, Satin J, Gepstein L. In vitro electrophysiological drug testing using human embryonic stem cell derived cardiomyocytes. *Stem Cells Dev*. 2009;18:161–172.
7. Germanguz I, Sedan O, Zeevi-Levin N, Shtrichman R, Barak E, Ziskind A, Eliyahu S, Meiry G, Amit M, Itskovitz-Eldor J, Binah O. Molecular characterization and functional properties of cardiomyocytes derived from human inducible pluripotent stem cells. *J Mol Cell Med*. 2011;15:38–51.
8. Sedan O, Dolnikov K, Zeevi-Levine N, Fleishmann N, Amit M, Itskovitz-Eldor J, Binah O. 1,4,5-Inositol trisphosphate operated $[Ca^{2+}]_i$ stores and angiotensin-II/endothelin-1 signaling pathway are functional in human embryonic stem cell-derived cardiomyocytes. *Stem Cells*. 2008;26:3130–31388.
9. Shlapakova IN, Nearing BD, Lau DH, Boink GJ, Danilo P Jr, Kryukova Y, Robinson RB, Cohen IS, Rosen MR, Verrier RL. Biological pacemakers in canines exhibit positive chronotropic response to emotional arousal. *Heart Rhythm*. 2010;7:1835–1840.
10. Goldberger AL, Amaral LAN, Hausdorff JM, Ivanov PC, Peng CK, Stanley HE. Fractal dynamics in physiology: alterations with disease and aging. *Proc Natl Acad Sci U S A*. 2002;99(suppl 1):2466–2472.
11. Ivanov PC, Amaral LAN, Goldberger AL, Havlin S, Rosenblum MG, Struzik ZR, Stanley HE. Multifractality in human heartbeat dynamics. *Nature*. 1999;399:461–465.
12. McSharry PE, Malamud BD. Quantifying self-similarity in cardiac inter-beat interval time series. *Comput Cardiol*. 2005;32:459–462.
13. Limat A, Noser FK. Serial cultivation of single keratinocytes from the outer root sheath of human scalp hair follicles. *J Invest Dermatol*. 1986;87:485–468.
14. Novak AR, Shtrichman R, Germanguz I, Segev H, Zeevi-Levin N, Fishman B, Mandel YE, Barad L, Domev H, Kotton DN, Mostoslavsky G, Binah O, Itskvitz-Eldor J. Enhanced reprogramming and cardiac differentiation of human keratinocytes derived from plucked hair follicles, using a single excisable lentivirus. *Cell Reprogram*. 2010;12:665–678.
15. Meiry G, Reisner Y, Feld Y, Goldberg S, Rosen M, Ziv N, Binah O. Evolution of action potential propagation and repolarization in cultured neonatal rat ventricular myocytes. *J Cardiovasc Electrophysiol*. 2001;12:1269–1277.
16. Little RC, Milken GA, Stroup WW, Wolfinger RD, Scabenberber O. *SAS for Mixed Models*. 2nd ed. Cary, NC: SAS Institute Inc; 2006.
17. Kobayashi M, Musha T. 1/f Fluctuation of heartbeat period. *IEEE Trans Biomed Eng*. 1982;29:456–457.
18. Huikuri HV, Mäkikallio TH, Peng CK, Goldberger AL, Hintze U, Moller M. Fractal correlation properties of R-R interval dynamics and mortality in patients with depressed left ventricular function after an acute myocardial infarction. *Circulation*. 2000;101:47–53.
19. Bigger JT Jr, Steinman RC, Rolnitzky LM, Fleiss JL, Albrecht P, Cohen RJ. Power law behavior of RR-interval variability in healthy middle-aged persons, patients with recent acute myocardial infarction, and patients with heart transplants. *Circulation*. 1996;93:2142–2151.
20. Huikuri HV, Makikallio TH, Airaksinen KE, Seppanen T, Puukka P, Raiha IJ, Sourander LB. Power-law relationship of heart rate variability as a predictor of mortality in the elderly. *Circulation*. 1998;97:2031–2036.
21. Pincus SM, Goldberger AL. Physiological time-series analysis: what does regularity quantify? *Am J Physiol*. 1994;266:H1643–H1656.
22. Iyengar N, Peng CK, Morin R, Goldberger AL, Lipsitz LA. Age related alterations in the fractal scaling of cardiac interbeat interval dynamics. *Am J Physiol*. 1996;271:R1078–R1084.
23. Kucera JP, Heuschkel MO, Renaud P, Rohr S. Power-law behavior of beat-rate variability in monolayer cultures of neonatal rat ventricular myocytes. *Circ Res*. 2000;86:1140–1145.
24. Ponard JG, Kondratyev AA, Kucera JP. Mechanisms of intrinsic beating variability in cardiac cell cultures and model pacemaker networks. *Biophys J*. 2007;92:3734–3752.
25. Kantelhardt JW, Koscielny-Bunde E, Rego HHA, Havlin S, Bunde A. Detecting long-range correlations with detrended fluctuation analysis. *Physica A: Statistical Mechanics and its Applications*. 2001;295:441–454.
26. Huikuri HV, Perkoimaki JS, Maestri R, Pinna GD. Clinical impact of evaluation of cardiovascular control by novel methods of heart rate dynamics. *Phil Trans R Soc A*. 2009;367:1223–1238.
27. Kamen PW, Krum H, Tonkin AM. Poincare plot of heart rate variability allows quantitative display of parasympathetic nervous activity in humans. *Clin Sci (Lond)*. 1996;91:201–208.
28. Bergfeldt L, Haga Y. Power spectral and Poincaré plot characteristics in sinus node dysfunction. *J Appl Physiol*. 2003;94:2217–2224.
29. Woo MA, Stevenson WG, Moser DK, Trelease RB, Harper RM. Patterns of beat-to-beat heart rate variability in advanced heart failure. *Am Heart J*. 1992;123:704–710.
30. Takens F. Detecting strange attractors in turbulence. In: Rand DA, Young LS, eds. *Dynamical Systems and Turbulence, Lecture Notes in Mathematics*. Volume 898. New York, NY: Springer; 1981.
31. Zimmerman MW, Povinelli RJ, Johnson MT, Ropella KM. A reconstructed phase space approach for distinguishing ischemic from non-ischemic ST changes using Holter ECG data. *Comput Cardiol*. 2003;30:243–246.
32. Heart rate variability: standards of measurement, physiological interpretation, and clinical use: Task Force of the European Society of Cardiology and the North American Society of Pacing and Electrophysiology. *Eur Heart J*. 1996;17:354–381.
33. Mäkikallio TH, Høiber S, Køber L, Torp-Pedersen C, Peng CK, Goldberger AL, Huikuri HV. Fractal analysis of heart rate dynamics as a predictor of mortality in patients with depressed left ventricular function after acute myocardial infarction: TRACE Investigators: TRAndolapril Cardiac Evaluation. *Am J Cardiol*. 1999;83:836–839.
34. Dori G, Denekamp Y, Fishman S, Rosenthal A, Lewis BS, Bitterman H. Evaluation of the phase plane ECG as a technique for detecting acute occlusion. *Int J Cardiol*. 2002;84:161–170.

35. Kehat I, Kenyagin-Karsenti D, Snir M, Segev H, Amit M, Gepstein A, Livne E, Binah O, Itskovitz-Eldor J, Gepstein L. Human embryonic stem cells can differentiate into myocytes with structural and functional properties of cardiomyocytes. *J Clin Invest*. 2001;108:407–414.

36. Mummery C, Ward-van Oostwaard D, Doevendans P, Spijker R, van den Brink S, Hassink R, van der Heyden M, Opthof T, Pera M, de la Riviere AB, Passier R, Tertoolen L. Differentiation of human embryonic stem cells to cardiomyocytes: role of coculture with visceral endoderm-like cells. *Circulation*. 2003;107:2733–2740.

CLINICAL PERSPECTIVE

Atrioventricular conduction block and arrhythmias caused by sinoatrial node dysfunction are generally treated with electronic pacemakers. Although an excellent therapy, electronic pacemakers incorporate limitations that have stimulated research on biological pacing. Initial proof of concept has been followed by attempts to optimize biological pacemakers so that their function of generating stable basal rates and brisk autonomic responses is manifested over long intervals. Importantly, the functional features of the prototypical biological pacemaker, the sinoatrial node, are not limited to automaticity. Rather, the normal node has an organized rhythm that is stable over time, imposes a dominant rhythm on the cardiac substrate, and has autonomic responsiveness. Hence, it is likely desirable that at least a subset of fabricated biological pacemakers would function much like the sinoatrial node. To achieve this, we need additional understanding of the intrinsic firing patterns of cell types proposed for use as biological pacemakers with the sinoatrial node as an operational standard. To this end, we recorded extracellular electrograms from human embryonic and induced pluripotent stem cell-derived cardiomyocytes, and the beat rate time series of the spontaneous activity were examined in terms of power spectral density and additional methods derived from nonlinear dynamics. In brief, we demonstrated that human embryonic and induced pluripotent stem cell–derived cardiomyocytes exhibit beat rate variability and power-law behavior as in humans, thus supporting the potential capability of these cell sources to serve as biological pacemakers.

Human Embryonic and Induced Pluripotent Stem Cell–Derived Cardiomyocytes Exhibit Beat Rate Variability and Power-Law Behavior

Yael Mandel, Amir Weissman, Revital Schick, Lili Barad, Atara Novak, Gideon Meiry, Stanislav Goldberg, Avraham Lorber, Michael R. Rosen, Joseph Itskovitz-Eldor and Ofer Binah

Circulation. 2012;125:883-893; originally published online January 18, 2012;
doi: 10.1161/CIRCULATIONAHA.111.045146
Circulation is published by the American Heart Association, 7272 Greenville Avenue, Dallas, TX 75231

Print ISSN: 0009-7322. Online ISSN: 1524-4539

SUPPLEMENTAL MATERIAL

SUPPLEMENTAL METHODS

Human embryonic and induced pluripotent stem cells-derived cardiomyocytes exhibit beat rate variability and power-law behavior

[a, b, c, *]Yael Mandel, [c, e, *]Amir Weissman, [a, b, c]Revital Schick, [a, b, c]Lili Barad, [a, b, c]Atara Novak, [a, b, c]Gideon Meiry, [a, b, c]Stanislav Goldberg, [d]Michael R Rosen, [a, c, e]Joseph Itskovitz-Eldor, [a, b, c]Ofer Binah

[a]The Sohnis Family Stem Cells Center, [b]The Rappaport Family Institute for Research in the Medical Sciences, [c]Ruth & Bruce Rappaport Faculty of Medicine, Technion - Israel Institute of Technology, Haifa, Israel, [d]Department of Pharmacology, College of Physicians and Surgeons of Columbia University, New York, USA. [e]Department of Obstetrics and Gynecology, Rambam Health Care Campus, Haifa, Israel.

Corresponding author

Ofer Binah, Ph.D.
Department of Physiology
Ruth & Bruce Rappaport Faculty of Medicine
POB 9649, Haifa, 31096 Israel
Email; binah@tx.technion.ac.il; Tel: +972-4-8295262; Fax: +972-4-8513919

*These autor contributed equally to the manuscript.

Methods

Generation of iPSC from human hair follicle keratinocytes

Derivation of keratinocytes from human plucked hair follicles

Ten hair follicles with visible outer root sheath were plucked from the scalp. The bulk of the hair follicles was cut off and the follicles were immersed in a 10 cm Petri dish with DMEM medium containing 25 mM HEPES, 1 mmol/L L-glutamine and 400 U/ml penicillin, 400 µg/ml streptomycin for 4-18 hrs in 37^{o}C. The follicles were washed with PBS, then covered with 0.1% trypsin and 0.02% EDTA (diluted with PBS) and incubated for 30 min at 37^{o}C. A single cell suspension culture was obtained by vigorously pipetting the follicles with DMEM supplemented with 10% FBS. The dissociated keratinocytes were centrifuged for 10 min at 200 g and seeded in 3 wells of a 6-well plate on an inactivated 3T3 feeder layer (2*10^{4} 3T3 cells/cm^{2}) with Green medium (60% DMEM, 30% DMEM F-12, 10% Fetal Bovine Serum, 1 mmol/L sodium pyruvate, 2 mM L-glutamine, 5 µg insulin, 0.5 µg/ml hydrocortisone, 0.2 nmol/L adenine, 2 nmol/L triiodothyronine (T3), 10 ng/ml Epidermal Growth Factor and 100 U/ml penicillin, 100 µg/ml streptomycin). For splitting, 3T3 cells were removed after incubation with 0.02% EDTA for 5 min in 37^{o}C. The culture was washed with PBS, after which the keratinocytes detached and were dissociated into signal cells by incubation with 0.1% Trypsin and 0.02% EDTA in PBS at 37°C for 10-15 min.[1]

Generation of iPSC from keratinocytes

On the first day 30,000 keratinocytes were seeded on an inactivated 3T3 feeder layer (20,000 cells/cm^{2}) supplemented with Green medium, in one well of a 6-well plate.[2] On the second day, viruses were produced as follows: The humanized version of a single lentiviral vector STEMCCA Cassette was generated following the transfection of 293T cells with five plasmids: STEM-CCA: Gag-Pol: REV: TAT: VSVG, at ratios of 20:1:1:1:2, respectively.[3] The total plasmid amount was 15 µg DNA. Transfection was done by a jetPEI™ Reagent (Polyplus

transfection™, France). The medium was replaced with a fresh one 24 hrs post-transfection (day 3). At 48 hrs post-transfection (day 4), the accumulated viral particles were filtrated through a 0.45 μm filter, supplemented with 2 μg/ml polybrene and used for infection of keratinocytes. Immediately before infection 3T3 feeder cells were removed using 0.02% EDTA. The infection was performed during centrifugation for 50 min with 500 g, at 32°C. Thereafter, the medium was replaced with fresh Green medium, and fresh inactivated 3T3 feeder cells were added. The infection was repeated on the following day (day 5). On day 5 post-infection (day 8) infected keratinocytes were detached by 0.1% Trypsin and 0.02% EDTA in PBS (Biological Industries, Beit Haemek, Israel) at 37°C for 10 min, centrifuged for 10 min at 200 g, and seeded on an inactivated mouse embryonic fibroblast (MEF) feeder with Green medium, in six wells of a 6-well plate. On the following day the medium was replaced with hESC medium containing 8 ng/ml bFGF (Invitrogen, N.Y, USA).[4] The medium was replaced every second day. Finally, 21-25 days after seeding the infected keratinocytes, hESC-like colonies emerged and could be further expanded and analyzed.

hESC and iPSC: culture and differentiation

hESC from clones H9.2 and iPSC were grown on mouse embryonic fibroblast feeders (MEF) in 80% knockout Dulbecco's modified Eagle's medium, 20% knockout serum replacement, 4 ng/ml basic fibroblast growth factor, 1 mmol/L glutamine, 0.1mmol/l β-mercaptoethanol, and 1% essential amino acid stock (all from Gibco-BRL, Gaithersburg, MD, http://www.gibcobrl.com).[5-8] To induce embryoid bodies (EBs) formation, hESC and iPSC were detached using 1 mg/ml type IV collagenase (Gibco-BRL) and transferred to Petri dishes to allow their aggregation. Resultant EBs were grown in 80% knockout Dulbecco's modified Eagle's medium, 20% fetal bovine serum defined (HyClone, Logan, UT, http://www.hyclone.com), 1 mmol/L glutamine, and 1% nonessential amino acid stock. The EBs were then cultured in suspension for 7 days and plated on gelatin-coated (0.1%;

Sigma-Aldrich, St. Louis, http://www.sigmaaldrich.com) 6-well plates. Daily microscopic observations were conducted to detect the first spontaneous contractions. The contracting areas were then carefully dissected out by microscalpel and transferred to fibronectin (1:20)-coated Micro-Electrode-Arrays (MEA).

Data recording and processing

The MEA set-up (Multi Channels Systems, MCS, Reutlingen, Germany) consists of a 50×50-mm glass substrate, in the center of which is embedded a 1.4×1.4 mm matrix of 60 titanium-nitride electrodes.[9, 10] The electrode diameter is 30 µm and inter-electrode distance is 200 µmol/L. Data were recorded at 10 kHz with 12-bit precision. Extracellular recordings from cultured hESC-CMs and iPSC-CMs were performed using a PC-based data acquisition system consisting of the MEA, preamplifiers, filter amplifier, data acquisition board and software. An additional PC was connected using an SD64 channel splitter to allow measurements using the BioBench software (National Instruments Inc., Austin, TX, USA). The signal was sampled at 500 Hz and stored in a binary file for off-line processing. The temperature of the MEA was kept at 37º±0.1ºC by means of temperature-maintaining system.[9, 10] For the 8-hrs recordings (long-term experiments) the MEAs were saturated with a gas mixture consisting of 5% CO_2 and 95% air.

The experimental protocols for testing the effects of isoproterenol and carbamylcholine

The experiments were performed on 17-25 day old spontaneously contracting hESC-CMs and iPSC-CMs. The MEAs were kept at 37^{o}C and equilibrated with a gas mixture of 95% CO_2 and 5% O_2. After recording control electrograms for 10 minutes, the preparations were exposed to ascending

concentrations (10 minutes recording at each concentration) of isoproterenol or carbamylcholine. After applying of the highest dose of isoproterenol or carbamylcholine, the preparations were exposed to isoproterenol + metoprolol or to carbamylcholine + atropine, respectively. Beat rate was calculated by measuring the number of action potentials during one minute at the time point of the maximal drug effect.

References

1. Novak A, Shtrichman R, Germanguz I, Segev H, Zeevi-Levin N, Fishman B, Mandel YE, Barad L, Domev H, Kotton D, Mostoslavsky G, Binah O, Itskovitz-Eldor J. Enhanced reprogramming and cardiac differentiation of human keratinocytes derivedrom plucked hair follicles, using a single excisable lentivirus. Cell Reprogram. 2010; 12:665-678.
2. Limat A, Noser FK. Serial cultivation of single keratinocytes from the outer root sheath of human scalp hair follicles. J Invest Dermatol. 1986; 87:485-468.
3. Mostoslavsky G, Fabian AJ, Rooney S, Alt FW, Mulligan RC. Complete correction of murine Artemis immunodeficiency by lentiviral vector-mediated gene transfer. Proc Natl Acad Sci U S A. 2006; 103:16406-11.
4. Thomson JA, Itskovitz-Eldor J, Shapiro SS, Waknitz MA, Swiergiel JJ, Marshall VS, Jones JM. Embryonic stem cell lines derived from human blastocysts. Science.1998; 282:1145-1147.
5. Itskovitz-Eldor J, Schuldiner M, Karsenti D, Eden A, Yanuka O, Amit M, Soreq H, Benvenisty N. Differentiation of human embryonic stem cells into embryoid bodies compromising the three embryonic germ layers. Mol Med. 2000; 6:88-95.
6. Dolnikov K, Shilkrut M, Gerecht-Nir S, Zeevi-Levin N, Ohayon D, Danon A, Itskovitz-Eldor, Binah O. Functional properties of human embryonic stem cell-derived cardiomyocytes: intracellular Ca^{2+} handling and the role of sarcoplasmic reticulum in the contraction. Stem Cells. 2006; 24:236-245.
7. Sedan O, Dolnikov K, Zeevi-Levin N, Fleishmann N, Amit M, Itskovitz-Eldor J, Binah O. 1,4,5-Inositol trisphosphate operated $[Ca^{2+}]_i$ stores and angiotensin-II/endothelin-1 signaling pathway are functional in human embryonic stem cell-derived cardiomyocytes. Stem Cells.2008; 26:3130-3138.

8. Germanguz I, Sedan O, Zeevi-Levin N, Shtrichman R, Barak E, Ziskind A, Eliyahu S, Meiry G, Amit M, Itskovitz-Eldor J, Binah O. Molecular characterization and functional properties of cardiomyocytes derived from human inducible pluripotent stem cells. In Press in: J Mol Cell Med. 2011; 15:38-51.

9. Meiry G, Reisner Y, Feld Y, Goldberg S, Rosen M, Ziv N, Binah O. Evolution of action potential propagation and repolarization in cultured neonatal rat ventricular myocytes. J Cardiovasc Electrophysiol. 2001; 12:1269-1277.

10. Reisner Y, Meiry G, Zeevi-Levin N, Barac DY, Reiter I, Abassi Z, Ziv N, Kostin S, Schaper J, Rosen MR, Binah O. Impulse conduction and gap junctional remodelling by endothelin-1 in cultured neonatal rat ventricular myocytes. J Cell Mol Med. 2009; 13: 562-573.